

$\psi' \rightarrow \psi \pi \pi$ decay as a test of partial conservation of axial-vector current

D. Morgan and M. R. Pennington

Rutherford Laboratory, Chilton, Didcot, Berkshire, OX11 0QX, England

(Received 14 April 1975)

The shape of the $\pi^+ \pi^-$ mass distribution in the recently analyzed $\psi' \rightarrow \psi \pi \pi$ decay is explained. Although the explanation assumes the known general features of the $\pi \pi$ s -wave amplitude, detailed alternatives are not distinguished; rather, it is the on-shell appearance of the Adler zero which is crucial. The extension of this description to other dipion production processes is illustrated with a discussion of low energy $\pi^- p \rightarrow \pi^+ \pi^- n$.

The recent discovery of the ψ and ψ' resonances¹ provides the opportunity to study familiar hadron systems in novel situations. A notable example is the cascade decay $\psi' \rightarrow \psi \pi \pi$ (Ref. 2) which seems to offer an instance of $I=0$ s -wave dipion production of unrivalled purity. The associated $\pi \pi$ mass distribution presents a very similar appearance to those seen in low-energy $\pi N \rightarrow \pi \pi N$ processes. Such mass distributions are often directly identified with the corresponding $\pi \pi \rightarrow \pi \pi$ parameters, although, as is well known, this is quite unjustified. The correct interrelationship with the four-pion amplitude is much more indirect, and the potential for learning about $\pi \pi$ scattering is therefore very restricted. Indeed, as we shall see, such reactions constitute first and foremost a test of PCAC (partial conservation of axial-vector current).

As already implied, we shall assume that the pions appearing in the $\psi' \rightarrow \psi \pi^+ \pi^-$ decay are produced in an $I=J=0$ state, just as present experiments indicate. It is, however, important to confirm this quantum number assignment³: to check for the absence of appreciable $I=2$ components from the $\pi^+ \pi^- / \pi^0 \pi^0$ branching ratio, and for the absence of higher spin states from the observed decay angular distributions. The narrow ψ and ψ' decay widths indicate that these particles do not interact strongly with other presently known hadrons, in particular with the pions appearing in the cascade decay. The dynamical structure of the decay is thus entirely given by the final-state interaction of the outgoing pions. The amplitude is then described by the appropriate scalar form factor of the pion, $F_\psi(t)$, just as $e^+ e^- \rightarrow \pi^+ \pi^-$ scattering measures the pion's electromagnetic form factor, $F_{em}(t)$.

The observed decay distribution, $d\sigma/dM_{\pi\pi}$, of Ref. 2 (the shape of which is indicated in Fig. 1), is related to $F_\psi(t)$ by

$$\begin{aligned} \frac{d\sigma}{dM_{\pi\pi}} &= (\text{normalization constant}) \\ &\times (\text{phase space} \times \text{acceptance}) \\ &\times |F_\psi(t)|^2, \end{aligned} \quad (1)$$

where $t = M_{\pi\pi}^2$ and lies in the range $4\mu^2 \leq t \leq (M_{\psi'} - M_\psi)^2$. A pion form factor $F(t)$ is, quite generally, a real analytic function in the complex t plane, cut from 2π threshold at $t = 4\mu^2$ to $+\infty$.

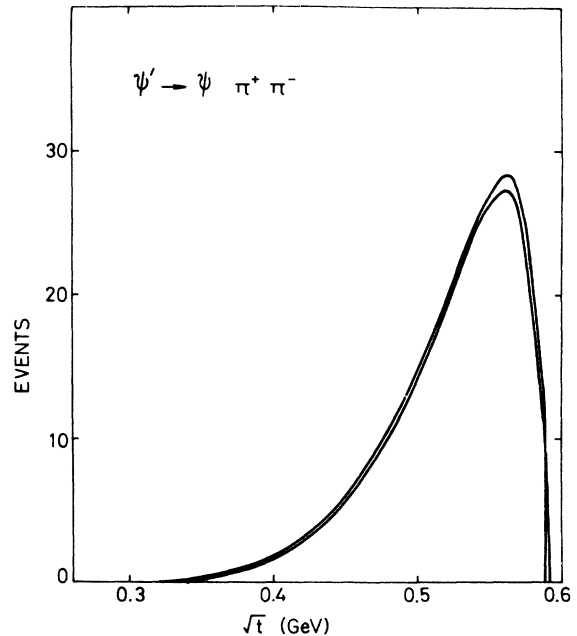


FIG. 1. Form of the $\pi \pi$ mass spectrum in $\psi' \rightarrow \psi \pi^+ \pi^-$ decay. The experimental data of Ref. 2 is here represented by two examples of our fittings [cf. Fig. 2(a)] using the form factor prescription outlined in the text. For details of the experimental mass distribution and acceptances see Fig. 7 of Ref. 2.

Defining the phase of $F(t)$ to be $\phi(t)$, the form factor satisfies the standard Omnès-Muskhelishvili representation⁴

$$F(t) = P(t)\mathfrak{D}^{-1}(t), \quad (2)$$

where the Omnès function is given by

$$\mathfrak{D}(t) = \exp \left[\frac{-t}{\pi} \int_{4\mu^2}^{\infty} dt' \frac{\phi(t')}{t'(t'-t)} \right] \quad (3)$$

and the polynomial $P(t)$ contains the zeros, if any, of the form factor. Calculating \mathfrak{D} from (3) entails fixing the form of ϕ . Below the inelastic threshold, this is accomplished via Watson's final-state interaction theorem,⁵ according to which ϕ equals the corresponding $\pi\pi$ elastic phase shift; once inelasticity enters, we will have to construct models for the phase.

In general, the structure of the form factor is controlled by the interplay of the polynomial $P(t)$ with the Omnès \mathfrak{D} function. In the familiar case of the pion electromagnetic form factor, the polynomial P varies slowly, corresponding to the absence of nearby zeros, so that it is the \mathfrak{D} function alone which describes the variation of $F_{em}(t)$. Moreover, this Omnès function is of a particularly simple form, being dominated by the ρ resonance; as a result, $F_{em}(t)$ closely resembles the corresponding $I=J=1$ $\pi\pi$ amplitude. This similarity is a special consequence of there being a dominant nearby pole and no nearby zeros.

With F_ψ and other s -wave form factors the roles of the two contributions are, as we shall see, completely reversed. On the one hand, $\mathfrak{D}(t)$, lacking the imprint of any conspicuous low-energy resonance pole, varies rather mildly; on the other hand, $P(t)$ turns out to be dominated by a zero near threshold, which may be interpreted as the on-shell counterpart of the off-shell Adler zero. It is for this reason that processes such as $\psi' \rightarrow \psi\pi\pi$ decay, which are governed by s -wave pion form factors, do not readily yield information on the low-energy $\pi\pi$ phase shifts. A spurious predictiveness is achieved if an isobar model or final-state interaction type of approximation, $F \propto e^{i\delta_{\pi\pi}} \sin \delta_{\pi\pi} / q_{\pi\pi}$, is adopted,⁶ since this forces the form factor zero to coincide with that of the elastic scattering amplitude. Although yielding the correct phase, such an identification is quite unfounded, except for the special situation, already discussed, typified by $F_{em}(t)$. In the situation of $\psi' \rightarrow \psi\pi\pi$ decay, where the polynomial is the rapidly varying component of the form factor, it is the zeros, their existence and positions, which are the principal outcome of the analysis. Since PCAC is so successful in other pion processes,⁷ we have the overwhelming expectation that here, too, the

scalar form factor will have a near-threshold zero. Whether this expectation is justified is for experiment to say.

To accomplish this test of PCAC we need, in effect, to form the product $F_\psi(t) \mathfrak{D}(t)$ of Eq. (2) in order to examine the structure of the experimental $P(t)$. This requires our building models for the phase, $\phi(t)$, so that we can compute the Omnès \mathfrak{D} function according to Eq. (3).

Using our assumption of only an s -wave $\pi\pi$ interaction, we know rigorously that for $t < 16\mu^2$, $\phi(t) = \delta_0^0(t)$.⁸ Above $16\mu^2$, we consider two distinct classes of model for the phase, both of which smoothly continue into $\delta_0^0(t)$ as $t \rightarrow 16\mu^2$.

Model (a): The first scheme is to assume that the phase of F_ψ continues to equal that of the $\pi\pi$ s -wave amplitude, i.e., $\phi = \phi_A \equiv \arg(T_{\pi\pi})$, so that

$$\tan \phi_A(t) = \frac{1 - \eta_0^0(t) \cos 2\delta_0^0(t)}{\eta_0^0(t) \sin 2\delta_0^0(t)}. \quad (4)$$

Model (b): The second possibility is that proposed by Barton in Ref. 8, which takes account of the coupled inelastic channels in an alternative way. This prescription gives $\phi = \phi_B \equiv \arg(\frac{1}{2} + \frac{1}{2}S_{\pi\pi})$, so that

$$\tan \phi_B(t) = \frac{\eta_0^0(t) \sin 2\delta_0^0(t)}{1 + \eta_0^0(t) \cos 2\delta_0^0(t)}. \quad (5)$$

A feature of both these models is that the phase ϕ is determined by the $\pi\pi$ s -wave amplitude.⁹ Below 900 MeV, we have chosen three possibilities for this partial wave which span the gamut of our phenomenological expectations, i.e., solutions to the Roy equations found by Basdevant *et al.*¹⁰ with scattering lengths of $a_0^0 = -0.05, 0.17,$ and $0.59 \mu^{-1}$, respectively.¹¹ From 900 to 1890 MeV, we use the $I=0$ s -wave amplitude extracted from the CERN-Munich data¹²: To be specific, we quote results using the analysis of Ochs and Wagner,¹³ although switching to that of Männer¹⁴ or Estabrooks and Martin¹⁵ makes negligible difference, since we are only concerned with the \mathfrak{D} function for $\sqrt{t} < 600$ MeV.

Equations (4) and (5), of course, only define the phases ϕ_A or ϕ_B modulo π ; which sector the phase is in is determined by continuity. Nonetheless, four separate possibilities naturally arise which lead to corresponding variations in the asymptotic behavior of ϕ .

Model (a): ϕ_A . Phenomenologically $\eta_0^0 = 1$ up to $K\bar{K}$ threshold. However, there is ambiguity as to whether the phase δ_0^0 reaches 180° before inelasticity sets in or not. Clearly, two possibili-

ties result: Either $\eta < 1$ when $\delta_0^0 = 180^\circ$, in which case ϕ_A is confined to the range $\phi_A \in [0, \pi]$ for all t , so that ϕ_A asymptotes to some value in this region; or, less likely, $\eta = 1$ when $\delta_0^0 = 180^\circ$, so that ϕ_A also passes through 180° . In this latter case, ϕ_A is trapped above the effective inelastic threshold between π and 2π and asymptotes accordingly.¹⁶

Model (b): ϕ_B . Two possibilities also arise here. However, it is whether $\eta = 1$ or $\eta < 1$ when $\delta_0^0 = 90^\circ$ (rather than 180°) which is now critical—in all phase-shift analyses, inelasticity has definitely set in by the time δ_0^0 reaches 270° . Phenomenologically, $\eta_0^0 = 1$ when δ_0^0 passes through 90° at around 900 MeV , so that, above the effective inelastic threshold, $\frac{1}{2}\pi \leq \phi_B \leq \frac{3}{2}\pi$. Despite this phenomenological result, we know that there must be at least a microscopic amount of inelasticity by 900 MeV when δ_0^0 reaches 90° ; according to this consideration, ϕ_B is always trapped between $-\frac{1}{2}\pi$ and $+\frac{1}{2}\pi$ and asymptotes accordingly.

As already mentioned, the \mathfrak{D} functions of Eq. (3) resulting from these possibilities for $\phi(t)$ are all very slowly varying for \sqrt{t} between 2π threshold and $(M_{\psi'} - M_\psi) = 590 \text{ MeV}$, as illustrated in Figs. 2(b)–2(d). Having constructed a range of possibilities for \mathfrak{D} and knowing $|F_\psi|$ from the experimental data, we are now in a position to determine the polynomial $P(t)$, in which we hope to see the PCAC zero. $P(t)$ is indeed very well fitted by a linear function of t . Representative forms for $|F_\psi(t)|$ are shown in Fig. 2(a), where, as throughout, purely statistical errors are assumed. We find for our extreme forms of \mathfrak{D} (the corresponding fits to the experimental mass distribution are shown in Fig. 1) that the zero, $t_0 \equiv t_0^\psi$, of the form factor lies between $2.5\mu^2 \leq t_0 \leq 6\mu^2$ with $t_0 \in [3.7, 5.5] \mu^2$ most strongly favored. It is the existence of this zero and the above determination of its position which is our main result.

The claim that this zero is the on-shell manifestation of the Adler zero can be understood quite simply. Weinberg¹⁷ has discussed the implications of current algebra and PCAC for pion scattering off any target: $\pi(k_1)A(p_1) \rightarrow \pi(k_2)B(p_2)$ (since crossing symmetry is a feature of such a discussion, all the crossed processes such as $A\bar{B} \rightarrow \pi\pi$ are also included). Weinberg argues that the low-energy amplitude, continued off-shell in the pion momenta, can be expressed as a sum of the following four terms:

$$\begin{aligned} \mathfrak{M} = & \text{Born term} + (\text{calculable current-algebra term}) \times (p_1 + p_2) \cdot k, \\ & + \mathfrak{M}_\sigma \text{ (the matrix element of the } \sigma \text{ commutator)} + (\text{terms quadratic in the pion momenta}). \end{aligned}$$

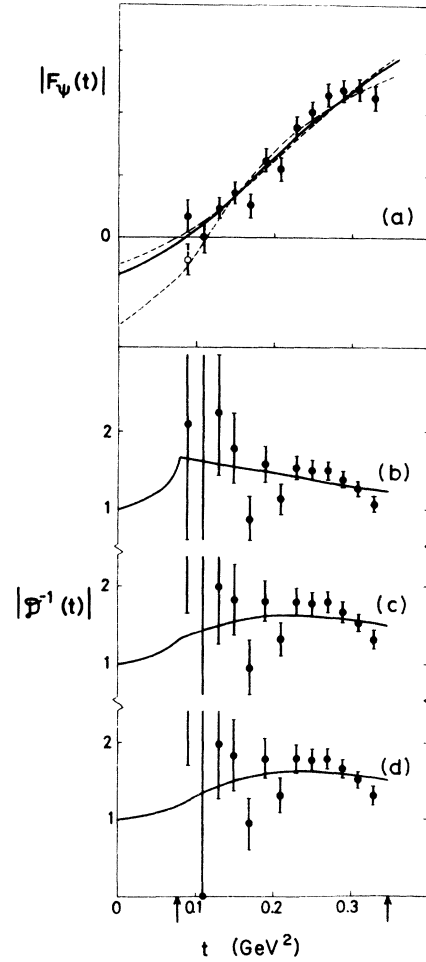


FIG. 2. The form factor and its constituent inverse \mathfrak{D} function are plotted as functions of t . (a) The modulus of the form factor, $|F_\psi|$ (strictly $F_\psi e^{-i\phi}$), extracted from the experimental data using Eq. (1). In constructing the lowest-energy data point we have allowed a sign ambiguity as shown. The curves depict our fits to this data. The dashed curves represent the two extreme possibilities, while the solid curve is a typical fit. (b)–(d) The modulus of the calculated inverse Omnès \mathfrak{D} function, corresponding to scattering lengths (b) $0.59 \mu^{-1}$, (c) $0.17 \mu^{-1}$, and (d) $-0.05 \mu^{-1}$, is compared with the experimental form factor of (a) divided by the appropriate fitted zero [c.f. Eq. (2)]. Note the marked effect of 2π threshold. The examples shown all correspond to the model $\phi = \phi_A$ with $\phi_A(\infty) = \frac{1}{2}\pi$, Eq. (4). The arrows on the abscissa mark the limiting values of phase space, viz. $t = 4\mu^2$ and $t = (M_{\psi'} - M_\psi)^2$.

The first two terms, where present as in πN scattering, dominate the scattering amplitude in the near threshold region. This is because the σ and quadratic terms are both supposedly very much smaller, being proportional to μ^2/M_A^2 . In the case of $\pi\psi' \rightarrow \pi\psi$ scattering,¹⁸ the first two terms of Eq. (6) are, in fact, absent: (i) because there are no strong-interaction Born terms; and (ii) because of Bose statistics. For low pion momenta, we can therefore expand the matrix element \mathfrak{M} , being just the sum of σ and quadratic terms, as

$$\mathfrak{M} = 2\alpha k_1 \cdot k_2 + \beta(k_1^2 + k_2^2 - \mu^2) + \gamma. \quad (7)$$

As required, the amplitude is symmetric in the two pion momenta k_1 and k_2 . On mass shell, this gives

$$\mathfrak{M}_{\text{on-shell}} = \alpha(t - 2\mu^2) + \beta\mu^2 + \gamma. \quad (8)$$

Now let us impose the Adler condition on the off-shell amplitude of Eq. (7). This requires the amplitude to vanish when either k_1 or $k_2 \rightarrow 0$; this demands $\gamma = 0$. (This also implies that $\mathfrak{M}_0 = -\beta\mu^2$; this proportionality of \mathfrak{M}_0 to μ^2 is just what we would expect, since setting $\mu = 0$ is believed to require conservation of the axial-vector current, which in turn implies $\mathfrak{M}_0 = 0$ in a truly massless pion world). In general, the parameters α and β are unrelated (and of course process-dependent), and can only be determined by very specific models or by experiment. Nonetheless, we do expect α and β to be of the same order. What the Adler condition has achieved is to secure the vanishing of the constant γ , first in the off-shell expansion, and thence in the on-shell amplitude of Eq. (8). We are thus led to expect this latter amplitude to vanish at $t = O(\mu^2)$, although the exact position of the zero is not predicted. As we have seen, this qualitative expectation is upheld by the data.

The result of our analysis has been that the $\pi\pi$ mass distribution of the $\psi' \rightarrow \psi\pi\pi$ decay is dominated by the PCAC zero near threshold with rather a weak dependence on the details (as opposed to the general behavior) of the $\pi\pi$ s -wave amplitude. Were we to be independently given the position of the zero, $F_\psi(t)$ could be used to discriminate between different \mathfrak{D} functions and, in particular, between different s -wave scattering lengths. The differences between the various \mathfrak{D} functions are most pronounced close to threshold, Figs. 2(b)–2(d). One might suppose that with a significant improvement in statistics different $\pi\pi$ phase shifts could be distinguished. To check on this, we will look at the $\pi\pi$ mass distribution in the process $\pi^- p \rightarrow \pi^+ \pi^- n$ close to threshold. Although this reaction is complicated by other than final-state $\pi^+ \pi^-$ strong interactions, let us assume for the sake of illustration

that it too is described by a scalar form factor, which we denote by $F_N(t)$. Just as for the corresponding $\psi' \rightarrow \psi\pi^+ \pi^-$ decay amplitude, we would expect it to be dominated by the zero corresponding to PCAC, although its on-shell location will in general be different. While the present ψ' decay data only provide a couple of events in the crucial near-threshold region, the data of Jones *et al.*¹⁹ on $\pi N \rightarrow \pi\pi N$ give almost a thousand events at each of two different pion momenta close to threshold. This latter reaction, with the above simplifying assumptions, therefore provides us with an ideal testing ground, not only for checking the Omnès representation itself, but also for distinguishing different $\pi\pi$ phase shift solutions. The result is somewhat surprising. As hoped, the appropriate scalar pion form factor $F_N(t)$ computed from the published mass distributions is excellently described by the Omnès representation, Fig. 3. However, notwithstanding the very considerable experimental precision, these very good fits are obtained for the whole range of possibilities for the $\pi\pi$ s -wave amplitude described above, with scattering lengths ranging from -0.05 to $+0.59 \mu^{-1}$. For each initial πN energy, the PCAC zero is well located, being at $t_0 = (3.6 \pm 0.3)\mu^2$ for $p_L = 415$ MeV/c and at $t_0 = (2.6 \pm 0.3)\mu^2$ at $p_L = 456$ MeV/c. Although the \mathfrak{D} function close to threshold changes appreciably as the scattering length is varied (cf. Fig. 2), the persistently good agreement of $\chi^2 = 0.6$ per data point is obtained by small adjustments in the

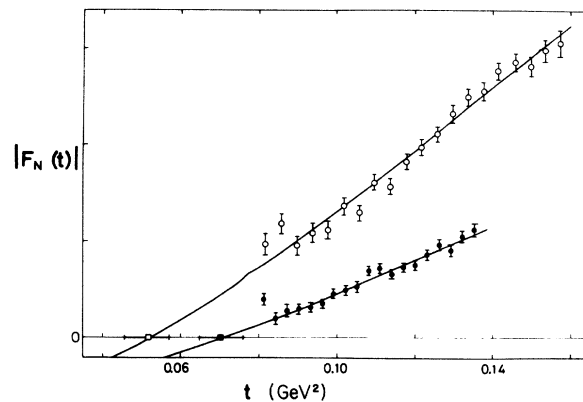


FIG. 3. The form factor $|F_N(t)|$ extracted from low-energy $\pi^- p \rightarrow \pi^+ \pi^- n$ data of Ref. 19, assuming the model of Eq. (1). The closed points correspond to $p_L = 415$ MeV/c and the open ones correspond to $p_L = 456$ MeV/c. The curves show typical examples of our fits to this data. Again note the kink occurring at 2π threshold. The corresponding zero position of these fits is denoted by solid and open squares, respectively. The error bands on these zero positions mark the full range of possibilities obtained with the models discussed in the text.

position of the near threshold zero. The differing positions of the zeros of F_N at the two momenta may perhaps be attributed to the altered kinematics or to reflections of other neglected hadronic processes.

With increasing reservations about the other neglected interactions, one can extend a similar description to the $(\pi^+\pi^-\pi^0)$ decay modes of the η and K_L^0 . Such an analysis gives each zero considerably displaced from those discussed above. Based on the data of Refs. 20 and 21, their respective locations, t_0^η and t_0^K , are found to be in the vicinity of $-\mu^2$ and $0.3\mu^2$, where t_0^η is not very well determined.

For each of the reactions we have considered, it is the on-shell manifestation of the Adler zero which is the controlling parameter. Indeed, it is the exact location of this zero (as yet uncertain) in the $\pi\pi$ s -wave amplitude itself, which completely determines the behavior of the low-energy $\pi\pi$ amplitude. Knowledge of the position of this zero would remove the effective one-parameter ambiguity in phenomenological analyses based on fixed- t dispersion relations and the Roy equations,¹⁰ and so provide a unique extrapolation to threshold.²² However, while the positions of all these zeros are $O(\mu^2)$, their exact location is seen to depend both on the particular process and on its kinematic configuration. We may hope that theoretical models will be developed to predict and explain accurately this detailed variation.²³

It is, of course, this variability of t_0 from reaction to reaction, together with the comparative featurelessness of the Omnès \mathfrak{D} function at low energies, which frustrates attempts to infer $\pi\pi$ elastic phase shifts from the related processes we have been considering. Both these obstacles lessen as the available range of dipion mass is

extended, and, once the region $M_{\pi\pi} \simeq 1$ GeV is encompassed, one would expect to observe a sharp S^* peak in the mass spectrum.²⁴ Indications of such a peak, preceded by a pronounced dip, have already been reported for the reaction $\bar{p}p_{\text{at rest}} \rightarrow \omega\pi^+\pi^-$.²⁵ An analogous situation, hopefully more clear cut because $I_{\pi\pi}$ must be zero³ rather than being merely favored, should arise when data is available on the decay mode $\psi \rightarrow \omega\pi^+\pi^-$ —although, as for the $\bar{p}p$ annihilation, the presence of three strongly interacting particles in the final state will complicate the interpretation. An exceptionally favorable circumstance would result if the reported bump at 4.15 GeV²⁶ should prove to have a $\psi\pi^+\pi^-$ decay mode. In all cases, achieved and envisaged,²⁷ the scope for learning about $\pi\pi$ phase shifts is strictly limited. It cannot be too strongly emphasized that quantitative progress in determining $\pi\pi$ amplitudes will almost certainly continue to come from the study of processes, such as K_{e4} and peripheral dipion production, where interfering phases (which do of course have a direct local relation to the corresponding elastic scattering parameters) are experimentally measured.

Our main conclusion is then as follows: The crucial feature characterizing reactions, such as $\psi' \rightarrow \psi\pi\pi$ decay, which are dominated by low-energy s -wave $\pi\pi$ interactions, is the on-shell appearance of the Adler zero. The shape of the experimental $\pi\pi$ mass distributions strongly support this belief in the PCAC hypothesis and underline its relevance for physical pion processes.

The authors thank the members of the LBL-SLAC collaboration, together with J. D. Jackson, for their help in making the experimental data available.

¹J. J. Aubert *et al.*, Phys. Rev. Lett. **33**, 1404 (1974); J.-E. Augustin *et al.*, *ibid.* **33**, 1406 (1974); G. S. Abrams *et al.*, *ibid.* **33**, 1453 (1974).

²G. S. Abrams *et al.*, in Proceedings of the Tenth Rencontre de Moriond, Méribel-les-Allues, France (to be published by CNRS) [also LBL Report No. LBL-3687, 1975 (unpublished)].

³That the $\psi'(3.7)$ and $\psi(3.1)$ are $I=0$ states and that their hadronic decays seemingly respect G parity are key constraints on any successful theory of the new particles.

⁴R. Omnès, Nuovo Cimento **8**, 316 (1958); N. I. Muskhelishvili, Tr. Tbilis. Mat. Inst. im. A. M. Razmadze Akad. Nauk Gruz. SSR **10**, 1 (1941); in *Singular Integral Equations*, edited by J. Radok (Noordhoff, Groningen, The Netherlands, 1953).

⁵K. M. Watson, Phys. Rev. **88**, 1163 (1952).

⁶The $I=0$ s -wave $\pi\pi$ amplitude is parametrized by

$$T_{\pi\pi} \equiv \frac{1}{2i\rho} (S_{\pi\pi} - 1) = \frac{1}{2i\rho} (\eta_{\pi\pi} e^{i\delta_{\pi\pi}} - 1),$$

with the phase space $\rho = 2q_{\pi\pi}/M_{\pi\pi}$, and where $\eta_{\pi\pi} = \eta_0^0$ and $\delta_{\pi\pi} = \delta_0^0$.

⁷S. B. Treiman, in *Lectures on Current Algebra and Its Applications*, by S. B. Treiman, R. Jackiw, and D. J. Gross (Princeton Univ. Press, Princeton, 1972).

⁸G. Barton, *Introduction to Dispersion Techniques in Field Theory* (Benjamin, New York, 1965), pp. 143—150; the author attributes the prescription to M. L. Goldberger and S. B. Treiman.

⁹We assume as a working hypothesis that the range of models that we have considered encompass all likely possibilities. Note, however, that models (a) and (b)

both considerably restrict the range of options from that allowed on completely general grounds. The contingencies thereby excluded may be taken care of by the possible effects of distant zeros not included in $P(t)$.

¹⁰J. L. Basdevant, C. D. Froggatt, and J. L. Petersen, Nucl. Phys. B72, 413 (1974).

¹¹We actually use the solutions of Ref. 10 which are fitted to the "Berkeley" $I=0$ s -wave phase shifts [S. D. Protopopescu *et al.*, Phys. Rev. D 7, 1279 (1973)] since these occupy a central position among recent determinations.

¹²G. Grayer *et al.*, Nucl. Phys. B75, 189 (1974).

¹³B. Hyams *et al.*, Nucl. Phys. B64, 134 (1973).

¹⁴W. Männer *et al.*, in *Experimental Meson Spectroscopy—1974*, proceedings of the Boston Conference, edited by D. A. Garelick (A.I.P., New York, 1974), p. 22.

¹⁵P. Estabrooks and A. D. Martin, Nucl. Phys. B79, 301 (1974); Phys. Lett. 53B, 253 (1974).

¹⁶Assuming that η_0^0 never exactly returns to unity.

¹⁷S. Weinberg, Phys. Rev. Lett. 17, 616 (1966).

¹⁸To speak in this manner of the $\psi' \rightarrow \psi\pi\pi$ decay is merely a semantic convenience, the absence of strong $\pi\psi'$ and $\pi\psi$ interactions being, of course, central to our whole approach.

¹⁹J. A. Jones, W. W. M. Allison, and D. H. Saxon, Nucl.

Phys. B83, 93 (1974).

²⁰For an example of data on the $\eta \rightarrow 3\pi$ decay, see J. G. Layter *et al.*, Phys. Rev. D 7, 2565 (1973).

²¹For an example of data on $K_L^0 \rightarrow 3\pi$ decay, see G. Alexander *et al.*, Nucl. Phys. B65, 301 (1973).

²²There is a definite correlation between the $I=0$ s -wave scattering length a_0^0 and the corresponding zero position $t_0^{(e)}$. If a_0^0 is not too large, this relationship is approximately linear, being roughly given by $20a_0^0 \approx 4 - t_0^{(e)}$ (units $\mu=1$).

²³Such variations in the zero position occur even in very simple models, such as that in which the K_L^0 and η decays are pictured as proceeding by intermediate heavy "pions" with a simple Veneziano model ansatz for the final " π " $\rightarrow 3\pi$ vertex.

²⁴M. R. Pennington, Phys. Rev. D 6, 1458 (1972).

²⁵See R. Bizzarri *et al.*, Nucl. Phys. B14, 169 (1969).

²⁶J.-E. Augustin *et al.*, Phys. Rev. Lett. 34, 764 (1975).

²⁷This limitation would apply, for instance, to the two-photon processes $ee \rightarrow ee\pi\pi$. For a review of the possibilities with this reaction, see S. J. Brodsky, in Proceedings of the International Colloquium on Photon-Photon Collisions in Electron-Positron Storage Rings, Collège de France, Paris, 1973 [J. Phys. (Paris) Suppl. 35, C2-69 (1974)].